Glass Transition and Phase Diagrams of Strongly Interacting Binary Colloidal Mixtures

Amit Meller and Joel Stavans
Department of Electronics, Weizmann Institute of Science, Rehovot 76100, Israel
(Received 9 September 1991)

We used diffusing wave spectroscopy to determine the phase diagrams of binary mixtures of charge-stabilized colloidal particles of different dimensions in the low-screening limit. As the ratio of radii $r=r_1/r_2$ was increased progressively towards 1, the structure of the diagrams evolved from eutecticlike to azeotropiclike and finally to a diagram where complete solubility was found, much like in atomic systems. We present for the first time evidence for liquid-glass transitions in these strongly interacting systems as the relative composition of both species is varied.

PACS numbers: 82.70.Dd, 61.90.+d, 81.30.Dz

Suspensions of charge-stabilized spherical colloidal particles have been the object of numerous studies in recent years due in part to the many analogies that can be drawn between their behavior and that of simple atomic liquids and solids. Monodisperse colloidal suspensions show crystalline [1], liquid [2], and glassy phases [3] depending upon the solid volume fraction ϕ and the range κ^{-1} of the screened-Coulomb potential through which the particles interact. The (ϕ,κ^{-1}) phase diagram has been determined experimentally by x-ray [3] and light scattering [4]. Variational calculations [5] and molecular dynamics simulations [6] of the phase diagram have been made and good qualitative agreement was found with the experimental findings for $\phi<0.2$. One can push further the analogy between colloidal and atomic systems, and consider binary mixtures of colloidal particles of different radii. To characterize mixtures, two parameters are needed besides the total volume fraction ϕ and κ^{-1}: the ratio of sizes $r=r_1/r_2$ $(r<1)$ as well as the relative concentration of small particles $x=n_1/(n_1+n_2)$, where r_i (n_i) is the radius (number density) of particles of type i. Shear modulus measurements of mixtures as a function of x and interaction strength have revealed the existence of glassy behavior as evidenced by a finite shear modulus in the absence of Bragg scattering [7]. These colloidal glasses were metastable and formed ordered colloidal compounds showing Bragg scattering when allowed to equilibrate for months. The structure of the latter was studied by optical microscopy and different structures were obtained as a function of r, x, and ϕ [8]. Glass formation was also studied by observing the split in the second peak of structure factors of mixture suspensions [9], and a liquid-glass boundary was determined for a particular value of r. There are very few theoretical predictions concerning the global phase behavior of colloidal mixtures. Variational calculations of phase diagrams of mixtures for screened Coulomb potentials have been performed for different size ratios [10]. However, only crystal-liquid phase boundaries were determined. Molecular dynamics simulations have identified crystal, liquid, and glass phases but have dealt with particular values of x only [11,12]. To our knowledge, there has been no systematic experimental study of the phase behavior of mixtures and its dependence on r.

In this Letter we report results of light scattering experiments on binary mixtures of strongly interacting charged polystyrene spheres as a function of ϕ and x in the low-screening limit. We obtain phase diagrams for three different values of the size ratio r. We emphasize that these phase diagrams are not strictly equilibrium diagrams due to the metastability of the glassy phases we observe. To discern the difference in dynamical behavior between the different phases observed, we have used diffusing wave spectroscopy (DWS), a recently developed technique that probes the dynamics of multiple-scattering media [13]. Within DWS, the temporal correlation function $G(t)$ of the intensity of light scattered in the backscattering direction by noninteracting particles decays as $G(t)\sim\exp[-2\gamma(6t/\tau)^{1/2}]$ in the limit $L\gg l^*$, where L is the sample thickness and l^* is the photon mean free path. Here $\tau=(Dk^2)^{-1}$ is the time required for a scatterer with diffusion constant D to move one optical wavelength λ $(k=2\pi/\lambda)$, and $\gamma\sim2$. For a binary mixture of two monodisperse species of different size, τ is a weighted average of the individual values of the pure species [13]. MacKintosh and John have generalized DWS to the case of strongly interacting particles [14]. They have shown that for long photon paths, for which the transport of light is diffusive, $G(t)$ can be approximated by $G(t)\sim\exp\{-2\gamma[W(t)k^2]^{1/2}\}$ where $W(t)$ is the mean-square particle displacement. This result is valid provided the mean interparticle spacing d is larger than λ and the particle size. In our case there is at least a factor of 4 between d and the particle radii, while d and λ are comparable. Nonetheless, we will still use this result since the qualitative nature of the conclusions we draw will not be severely affected by our approximation. We stress that the value of γ may vary due to interaction effects. However, the square root singularity of $G(t)$ at short times is preserved in the presence of interactions [15]. Consequently, we expect that at short times the change in the slope of $G(t)$ with changing x is due mainly to a change in τ and not to a change in γ as in noninteracting samples [13]. We note that DWS has already been used to study

suspensions of correlated particles interacting via short-range hydrodynamic interactions [16].

Our experiments were performed with 1-mm-thick cells in a backscattering geometry. Light from a 488-nm laser equipped with a single-mode etalon [17] was beam expanded to form an incident plane source on the sample cell. Measurements were taken mainly in the perpendicular polarization with respect to the polarization of the incident beam, in order to select long photon paths and ensure diffusive transport. In addition, since long paths are selected, the scattering volume is essentially the whole sample, and thus we do not have to perform measurements over many scattering volumes to ensure good ensemble averages. This latter procedure is essential in quasielastic light scattering studies of nonergodic media in which nonergodicity leads to reduced relative intensity fluctuations in the scattered light [18]. The latter manifest themselves as reduced amplitudes of the normalized intensity correlation functions. Nevertheless, measurements on three widely spaced regions of our samples were made and averaged. Measurements were also taken with parallel polarization. Insofar as the structure of the phase diagrams is concerned, our results proved to be the same irrespective of the polarization. In order to compare correlation functions for different values of x, measurements were accumulated for nearly 1 h for each value of x, taking care that the counts on the first correlator channel coincided. The baseline was then subtracted and the data were normalized by the value of the first channel after the subtraction. The multiple sample-time option in our correlator enabled us to measure the baseline at sufficiently long times while probing short times with high resolution.

Mother samples of 10% mass fraction were deionized with ion-exchange resin after which strong iridescent colors appeared. Samples were made out of the mother samples with given relative concentration x and volume fraction ϕ. The samples were carefully introduced in the scattering cells five days after they were prepared, and measurements were taken 24 h later. In this work, we quote the bare physical dimensions of the particles. In principle, effective hard sphere diameters can be computed from the form of the potential, its range, and the charge of the particles. We have not done this since predictions based on these effective sizes fail to reproduce experimental results in the low-ionic-strength limit [4]. We therefore limit ourselves to quoting the charge for future reference. The latter was determined by conductivity measurements of samples obtained from the mother samples for different degrees of dilution as detailed by Schaefer [2]. We used polystyrene latex particles of nominal radii 0.067, 0.0865, 0.099, and 0.160 μm. The measured charges were $(1590 \pm 120)e$, $(2390 \pm 120)e$, $(3045 \pm 190)e$, and $(6640 \pm 330)e$, respectively. These values do not represent the total number of ionizable groups and reflect only the number groups with nonadsorbed counterions in the Stern layer. The dependence of the charge on the dimensions of the particles is to a good approximation quadratic.

In mapping (x,ϕ^{-1}) phase diagrams we determined the boundaries of crystalline phases by the presence or absence of Bragg scattering. No crystallographic information about the mixtures was obtained. The state of amorphous samples was determined by measuring $G(t)$. To illustrate our procedure we show $G(t)$ as a function of the square root of time for samples with $r=0.54 \pm 0.02$, $\phi=0.06$ ($\phi^{-1}=16.6$), and different values of x in Fig. 1. Actual measurements were made up to 152 $\sec^{1/2}\times 10^3$ in order to observe saturation effects in $G(t)$, however, only a reduced range is shown in Fig. 1 for the sake of clarity. For all the measurements the baseline was determined at around 1 sec. Starting with the crystal of small particles ($x=1$), the correlation function shows a fast decay for short times followed by a slowly decaying component which eventually saturates. This confirms our expectation that while particles in a crystal move relatively free for short times, they are confined to crystal sites and for long times their mean-square displacement $W(t)$ saturates. As x is decreased, Bragg scattering gradually disappears. In the present case, the iridescence is completely lost for $x=0.9$. The corresponding correlation function exhibits a long-time decay slower than that of the crystal due to the presence of the large particles. Thus particles are still confined to average positions [$W(t)$ saturates] while the sample is amorphous. Following previous authors [13], we call this a glass state. Note that the possible variation of γ with interactions which would be compatible with our data at short times cannot produce the saturation observed at long times. The be-

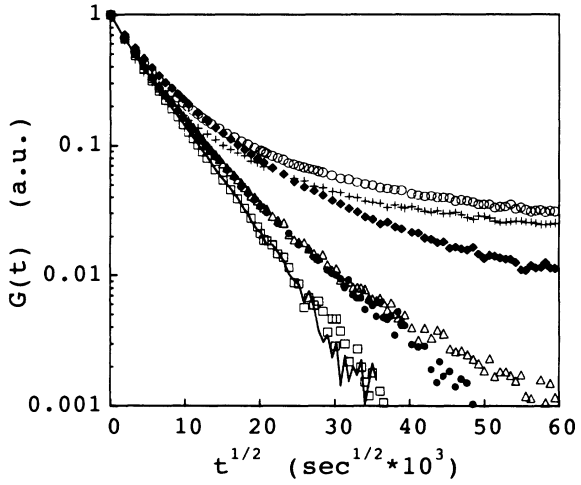

FIG. 1. Temporal autocorrelation functions of multiply scattered intensity $G(t)$ as a function of $t^{1/2}$ for $r=0.54$, $\phi=0.06$, and different values of the relative composition x: $x=1$ (crosses), $x=0.9$ (open circles), $x=0.7$ (open squares), $x=0.4$ (solid circles), $x=0.2$ (triangles), and $x=0$ (solid diamonds).

havior at $x=0.8$ is similar to that at 0.9 and is not shown for clarity. Decreasing x further to $x=0.7$, a sharp change occurs: The nondecaying long-time component disappears, and within the three decades spanned by our measurements the overall behavior becomes remarkably similar to that observed in systems of weakly interacting particles [13] *in spite of the strong interactions in the system.* We show by the solid line the correlation function obtained from a sample with the same values of ϕ and x in which the interactions have been screened. Indeed, the difference between the two data sets is very small. We thus call this a liquid state. Further decrease of x brings about a reversal of the trend just described: A slowly decaying component in $G(t)$ reappears for long times as can be noticed for $x=0.4$ and 0.2. The $x=0.2$ sample shows iridescence and a crystalline state is recovered. The reappearance of this long time scale is gradual in contrast to the sharp change between $x=0.8$ and 0.7 described above. Finally, we show $G(t)$ corresponding to the crystal of large particles ($x=0$).

In Fig. 2 we show three (x,ϕ^{-1}) phase diagrams with decreasing values of r. The solid lines, which serve as guides to the eye, are approximate boundaries between the crystal (open circles), glass (solid circles), and liquid (triangles) phases. In Fig. 2(a) which corresponds to $r=0.87\pm0.03$, both species are observed to be completely miscible in the crystalline state. The polydispersity of each species (of order 2%) whose effect becomes significant for r near 1, and the relatively small volume fractions involved, precluded a more precise determination of the melting points of the mixtures. The latter fall in the range $0.01\leq\phi\leq0.02$ for all values of x. Decreasing the size ratio to $r=0.78\pm0.04$ we observe complete solubility in the crystalline state provided ϕ is high enough, as shown in Fig. 2(b). There is a considerable depression of the melting point relative to that of the pure species. A glass phase appears which is limited to a narrow strip lying between the crystal and the liquid phases. We found difficulties in reproducing the glass boundaries in this case since the barriers for crystal nucleation are much lower than in the case of $r=0.54$ discussed below, and minor disturbances such as residual resin beads in the samples induced the formation of crystallites. Finally, we show in Fig. 2(c) a diagram corresponding to $r=0.54\pm0.02$. There are three salient features in this diagram. First, the melting point of the mixtures can reach values ($\phi\sim0.07$) which are even lower than in the two cases discussed above and are considerably lower than that of the pure species ($0.01\leq\phi\leq0.02$). Second, the asymmetry in the diagram is much more pronounced than that of Fig. 2(b), with the crystal phase on the $x=1$ side being smaller in extent than that of the $x=0$ side: It is easier to distort the lattice structure of the small particles by the addition of a few large ones than the opposite case when the size difference is large. By the same token, liquid-glass transitions on the $x=1$ side of the diagram are much sharper than those on the $x=0$ side, as previously illustrated in Fig. 1. Third, there is a miscibility gap in the crystalline state with the glass phase extending up to $\phi=0.1$, the highest volume fraction we studied. We estimate the error of the liquid-glass boundary to be about ±0.05 in x due to the difficulty in making a sharp distinction between the behavior of strongly interacting liquids and glasses particularly on the small-x side of the diagram. Though the extent of the glass phase seems to shrink as ϕ increases, it is unlikely for the miscibility gap to disappear for high enough ϕ since the pure species themselves are expected to form glasses above $\phi\sim0.15$ [3].

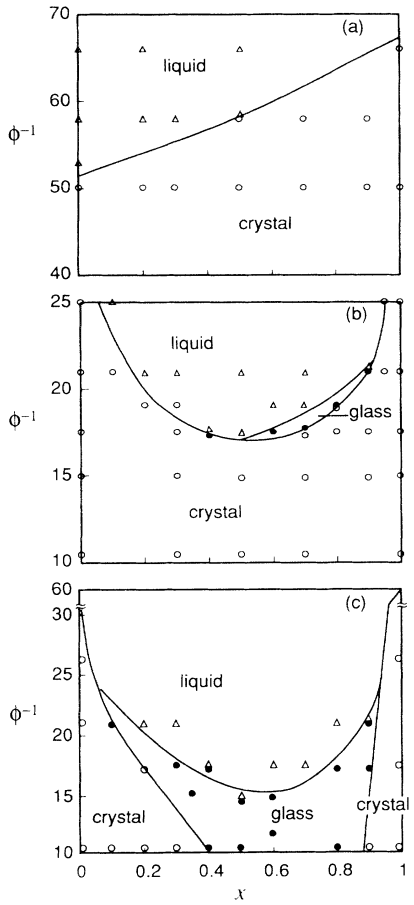

FIG. 2. Inverse volume fraction ϕ^{-1} vs relative concentration x phase diagrams for three values of the size ratio r: (a) spindle-type diagram ($r=0.87\pm0.03$), (b) azeotropic-type diagram ($r=0.78\pm0.04$), and (c) eutectic-type diagram ($r=0.54\pm0.02$). Solid lines between the liquid (triangles), glass (solid circles), and crystal (open circles) phases are just a guide to the eye.

Our measured phase diagrams reproduce many of the features observed in metallic systems such as alkali-metal mixtures [19]. Thus Fig. 2(a) resembles either a weak azeotrope or a spindle diagram, and is consistent with the

Hume-Rothery empirical criterion according to which complete solubility should be observed for $r > 0.85$. Figure 2(b) is similar to diagrams of azeotropic structure while Fig. 2(c), with the hornlike structure at intermediate values of ϕ, resembles a eutectic diagram. We have chosen values of r spanning a wide range of values in order to observe qualitative changes in the phase diagrams. However, any similarity between these values and those of real metals is fortuitous since our values of r have not been derived from interaction radii. Our phase diagrams have been plotted as a simple function of ϕ following previous authors [9–11]. A proper comparison with metallic systems would involve the osmotic pressure [20]. Our findings concerning the melting point depression are in good qualitative agreement with the predictions of variational calculations [10] and the structure of our diagrams follows the trend observed in density-functional calculations of hard-sphere mixtures [21]. It would be interesting to verify our findings using independent techniques such as small-angle x-ray scattering.

We thank S. Safran, V. Steinberg, E. Akkermans, and R. Klein for stimulating conversations. One of us (J.S.) thanks the Charles H. Revson Foundation for partial support of this work.

[1] P. Pieranski, Contemp. Phys. **24**, 25 (1983).
[2] J. C. Brown, P. N. Pusey, J. W. Goodwin, and R. H. Ottewill, J. Phys. A **8**, 664 (1975); D. W. Schaefer, J. Chem. Phys. **66**, 3980 (1977).
[3] E. B. Sirota, H. D. Ou-Yang, S. K. Sinha, P. M. Chaikin, J. D. Axe, and Y. Fujii, Phys. Rev. Lett. **62**, 1524 (1989).
[4] Y. Monovoukas and A. P. Gast, J. Colloid Interface Sci. **128**, 533 (1989).
[5] W. Y. Shih, I. A. Aksay, and R. Kikuchi, J. Chem. Phys. **86**, 5127 (1987).
[6] K. Kremer, G. S. Grest, and M. O. Robbins, Phys. Rev. Lett. **57**, 2694 (1986).
[7] H. M. Lindsay and P. M. Chaikin, J. Chem. Phys. **76**, 3774 (1982).
[8] S. Hachisu and S. Yoshimura, in *Physics of Complex and Supermolecular Fluids*, edited by S. A. Safran and N. A. Clark (Wiley, New York, 1987), p. 221.
[9] R. Kesavamoorthy, A. K. Sood, B. V. R. Tata, and A. K. Arora, J. Phys. C **21**, 4737 (1988).
[10] W. Y. Shih, W. H. Shih, and I. A. Aksay, J. Chem. Phys. **90**, 4506 (1989); W. H. Shih and D. Stroud, J. Chem. Phys. **80**, 4429 (1984).
[11] N. Pistoor and K. Kremer, in *Dynamics of Disordered Materials*, Proceedings of the ILL Workshop, Grenoble (Springer-Verlag, Berlin, 1989), p. 114.
[12] R. O. Rosenberg, D. Thirumalai, and R. D. Mountain, J. Phys. Condens. Matter **1**, 2109 (1989).
[13] D. J. Pine, D. A. Weitz, P. M. Chaikin, and E. Herbolzheimer, Phys. Rev. Lett. **60**, 1134 (1988); D. J. Pine, D. A. Weitz, J. X. Zhu, and E. Herbolzheimer, J. Phys. (Paris) **51**, 2101 (1990). See also G. Maret and P. E. Wolf, Z. Phys. B **65**, 409 (1987).
[14] F. C. MacKintosh and S. John, Phys. Rev. A **40**, 2383 (1989).
[15] D. J. Pine, D. A. Weitz, G. Maret, P. E. Wolf, E. Herbolzheimer, and P. M. Chaikin, in *Scattering and Localization of Classical Waves in Random Media*, edited by Ping Sheng (World Scientific, Singapore, 1990).
[16] S. Fraden and G. Maret, Phys. Rev. Lett. **65**, 512 (1990).
[17] T. Bellini, M. A. Glaser, N. A. Clark, and V. Degiorgio, Phys. Rev. A **44**, 5215 (1991).
[18] W. van Megen and P. N. Pusey, Phys. Rev. A **43**, 5429 (1991); P. N. Pusey and W. van Megen, Physica (Amsterdam) **157A**, 705 (1989).
[19] A. Voronel, S. Rabinovich, A. Kisliuk, V. Steinberg, and T. Sverbilova, Phys. Rev. Lett. **60**, 2402 (1988).
[20] P. Bartlett, J. Phys. Condens. Matter **2**, 4979 (1990).
[21] J. L. Barrat, M. Baus, and J. P. Hansen, Phys. Rev. Lett. **56**, 1063 (1986).